



JCSDA Quarterly

NOAA | NASA | US NAVY | US AIR FORCE

<https://doi.org/10.25923/4pt1-wx36>

IN THIS ISSUE

1 IN THIS ISSUE

Use of VIIRS Aerosol Optical Depth Information at NOAA GSL to Improve Smoke, Visibility, and Weather Forecasts in the Experimental High Resolution Rapid Refresh

Impacts of Aerosols on Simulated Brightness Temperature and Analysis Fields

Impacts of Aerosols on Meteorological Assimilation: A Case Study for the African Easterly Wave that Developed Hurricane Harvey

19 MEETING REPORT

20 PEOPLE

21 EDITOR'S NOTE

22 SCIENCE CALENDAR

22 CAREER OPPORTUNITIES

22 UPCOMING EVENTS

NEWS IN THIS QUARTER

Use of VIIRS Aerosol Optical Depth Information at NOAA GSL to Improve Smoke, Visibility, and Weather Forecasts in the Experimental High Resolution Rapid Refresh

Recent wildfires in the U.S. and abroad have underscored the far-reaching effects that smoke from wildfires has on lives and industries, impacting air quality, aviation, solar energy generation, and more. As a result, demand has increased for reliable and accurate forecasts of smoke emanating from wildfires. To address this need, the next operational implementation of the Rapid Refresh (RAP) and High-Resolution Rapid Refresh (HRRR) analysis and forecasting systems (planned for June 2020) will include, for the first time, a smoke prediction capability (Ahmadov et al., 2017).

In the 3-km resolution HRRR model, which covers the contiguous United States along with a separate Alaska domain, fire locations, sizes, and rate of biomass burning emissions are specified based on fire radiative power (FRP) observations. These observations are obtained from the MODIS instruments on the AQUA and Terra polar-orbiting satellites and from the VIIRS instruments on the Suomi-NPP (S-NPP) and NOAA-20 polar-orbiting satellites. To represent the smoke aerosol in the model, a single tracer has been added to HRRR via the coupling framework for the on-line WRF-Chem model (Grell et al., 2005). During model integration, the smoke tracer is mixed, advected, and deposited according to the model-predicted meteorology. In addition to the effects from the atmospheric field evolution on the model smoke field evolution, the model smoke aerosols also influence the meteorological fields through direct interaction with the radiation scheme. Critical to the success of these smoke prediction is smoke cycling: as new HRRR forecasts are initialized, the most recent valid forecast smoke field is inserted into the model initial conditions.

Disclaimer: The manuscript contents are solely the opinions of the author(s) and do not constitute a statement of policy, decision, or position on behalf of NOAA or any other JCSDA partner agencies or the U.S. Government.

**JOINT CENTER FOR SATELLITE
DATA ASSIMILATION**

5830 University Research Court
College Park, Maryland 20740

3300 Mitchell Lane
Boulder, Colorado 80301

Website: www.jcsda.org

EDITORIAL BOARD**Editor:**

James G. Yoe

Co-Assistant Editors:

Biljana Orescanin
Sandra L. Claar

Director:

Thomas Auligné

Chief Administrative Officer:

James G. Yoe

Thus, new smoke is continuously generated by fires that the most recent observations indicate are currently active, and existing modeled smoke fields continue to evolve through successive forecast runs.

Full descriptions of the RAP and HRRR smoke modeling capability and of the 2020 RAP and HRRR implementations are in preparation and will be reported elsewhere.

Improving HRRR Smoke Forecasts using Aerosol Optical Depth Measurements

Extensive experimentation has demonstrated the value of the smoke capability in improving surface visibility and temperature forecasts in regions where smoke is present, and the smoke diagnostics output in real-time by the experimental HRRR configuration maintained at NOAA/ESRL [<https://rapidrefresh.noaa.gov/hrrr/HRRRsmoke/>] have proven popular with users. Thus, it is important to continue to develop and improve upon this capability. In that vein, many upgrades are planned. One shortcoming of the current implementation is that, after smoke is injected based on observed FRP, no other observations directly impact the evolving smoke fields. In particular, no data representing smoke observations are ingested.

Model forecasts of three-dimensional smoke concentration fields, as well as forecasts of other model fields, stand to benefit from assimilation of observations that represent concentrations at all heights. One such data source is aerosol optical depth (AOD) derived from satellite observations. Specifically, NESDIS produces AOD and an accompanying Smoke Mask product, which flags pixels whose AOD is largely due to

smoke (rather than dust, ash, or cloud), using data from the S-NPP and NOAA-20 VIIRS instruments (Kondragunta et al., 2017; Zhou et al., 2019). These two products can be used in concert to identify model columns where little smoke should be present (where AOD is low) and others where high AOD is due to smoke concentration; at columns where the mask product indicates substantial presence of other aerosols, nothing should be inferred about the smoke concentrations.

To ingest AOD through a variational assimilation scheme, it is necessary to use a forward operator that converts the three-dimensional, model-predicted smoke concentration field into a simulated AOD measurement. Mariusz Pagowski has developed such an operator, along with its adjoint and tangent linear approximation, for use in the Gridpoint Statistical Interpolator (GSI). The operator has been demonstrated to improve forecast AOD in a WRF-Chem implementation with 20 km horizontal resolution (Pagowski et al., 2018). Experiments applying a variational approach for AOD data ingest to the current HRRR configuration will commence shortly at NOAA/ESRL.

In the interim, a short proof-of-concept experiment was conducted using a simplified approach that follows the HRRR's cloud clearing scheme (see Ladwig et al., 2020 and formal publication in preparation). In the cloud-clearing procedure, where observations indicate that no cloud is present, model-predicted clouds are removed from the HRRR grid boxes. This is accompanied by cloud building at grid points where observations indicate cloudiness. Whereas the cloud observations—cloud base height from ground-based sensors and cloud top

pressure from satellite—indicate height information for cloud building, similar observations indicating the height of smoke are not generally available. However, AOD data can be used to clear smoke from model columns where measured AOD values are low.

For this experiment, we make use of AOD detection by the S-NPP VIIRS only. At model initialization times when AOD data from S-NPP over the HRRR domain become available, at each grid column in the HRRR domain, if the maximum AOD reading within that column is less than 0.2 and every model grid box in the 5-grid-box by 5-grid-box surrounding area has some AOD readings (this excludes grid boxes near the edge of the AOD domain from being cleared), the cycled smoke field values at all the HRRR grid points in that model column are set to 0. At initialization times without new AOD data, the smoke field is cycled without modifications. As in the upcoming operational HRRR implementation, most model variables are initialized from the mean of the cycled HRRRDAS ensemble system (Ladwig et al., 2019), rather than cycled from the deterministic HRRR forecast. Therefore, fields such as temperature are identical between the control and experiment as the run initiates; all variation at later forecast hours is attributable to differences in the smoke field during model integration.

The test period for the simple AOD clearing experiment includes July 27th and 28th, 2018. During this time period, smoke from fires in California and Canada was transported throughout much of the contiguous United States and was dense in several western states. Between about 19 UTC and 21 UTC on the 27th, S-NPP

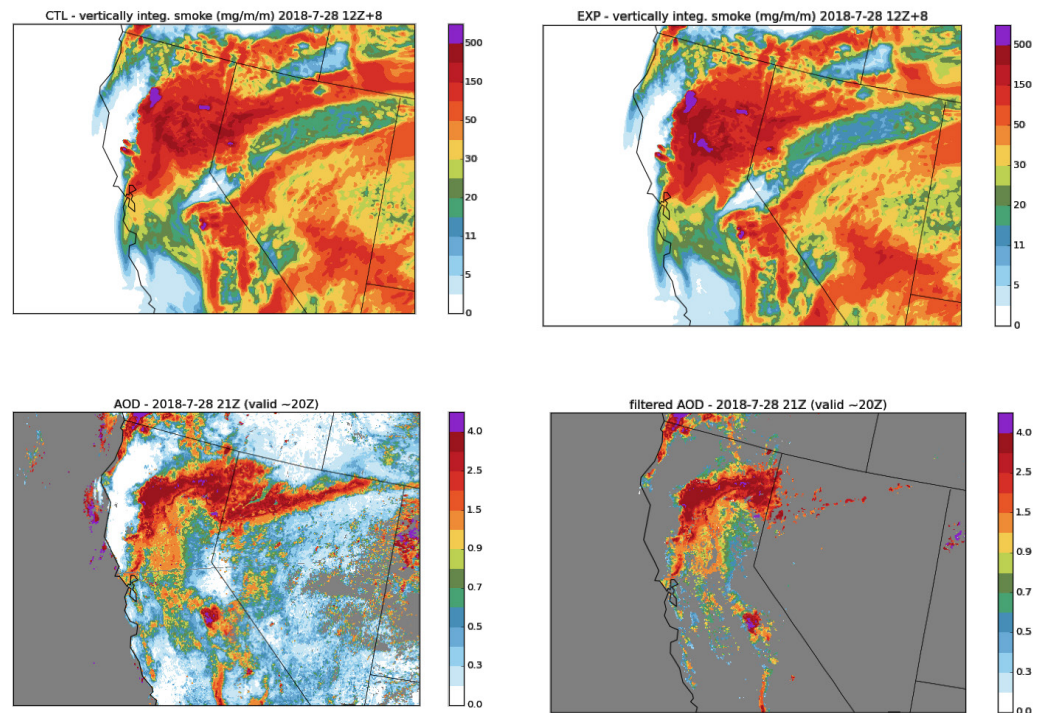
passes occurred first over Eastern CONUS, then over Western CONUS; AOD and smoke mask data from these passes were available for ingest into the 20 UTC and 22 UTC HRRR model initiations, respectively. For the experimental runs initiated at these two times, smoke clearing was performed as described above. In between and following these two hours of smoke clearing, the smoke was cycled as usual and all other observations, including FRP, were assimilated according to the usual HRRR configurations. The HRRR experiment was cycled forward until 12 UTC on the 28th; at 0 UTC and 12 UTC 12-hour forecasts were initiated. These forecasts were then compared with radiosonde observations valid at 12 UTC on the 28th and 0 UTC on the 29th.

At about 20 UTC on the 28th, S-NPP passed over the western United States again; AOD from this pass is displayed alongside the 8-hour HRRR control and experiment forecasts of vertically-integrated smoke concentration fields in *Figure 1*. In the experiment, smoke concentrations are decreased in a swath of Nevada leading into Idaho. In northern California, the smoke concentrations are decreased in some areas but increased in others as the smoke impacts on meteorology have caused changes to the smoke transport and accumulation.

Results of Proof-of-Concept Experiment

The two 12-hour forecasts produced, valid at 12 UTC on the 28th and 0 UTC on the 29th, were compared to 12-hour forecasts produced in a control run in which no smoke clearing was performed (but the model configuration was otherwise identical) and to observations by radiosondes launched

Figure 1. Top row: 8-hour forecasts of vertically integrated smoke (mg/m²)---valid 20 UTC on July 28, 2018, for the control (left) and experiment (right, using smoke clearing). Bottom row: AOD measured by S-NPP VIIRS at about 20 UTC on July 28, 2018; all AOD (left) and AOD filtered by NESDIS Smoke Mask (right). In the lower plots, grey indicates no measurement.



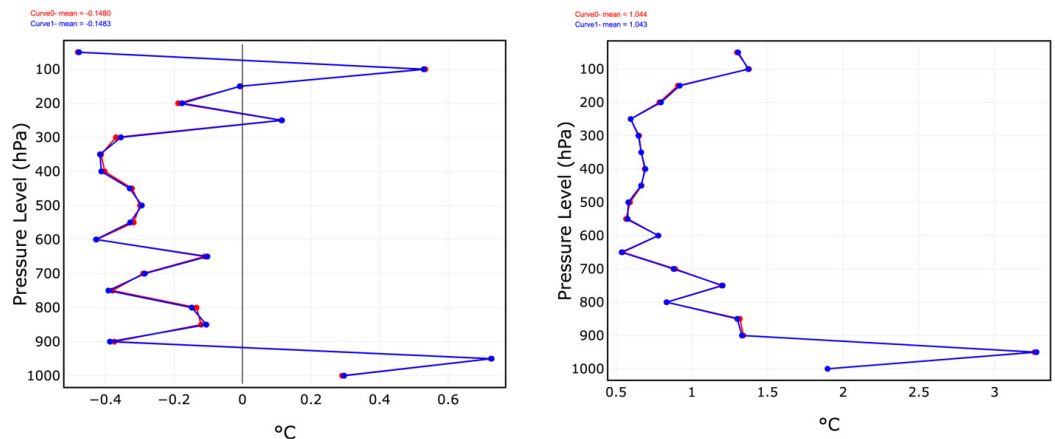
at those times over the western contiguous United States.

During the mostly nighttime hours between 0 and 12 UTC, the effect of varying smoke concentration on the meteorology, which is modulated by the feedback on radiation, is expected to be minimal. A comparison of smoke temperature forecast root-mean-squared error (RMS) and bias between the control and experiment, averaged over 75

radiosonde sites west of 109 W longitude, is shown in *Figure 2* and confirms that the differences in modeled smoke concentration had very little impact on the temperature forecasts.

In contrast, during the hours between 12 and 0 UTC, the feedback on radiation is expected to have a greater impact on temperature. The comparison of RMS and bias at 70 radiosonde sites west of 109 W

Figure 2. Temperature bias (left) and RMS (right) as a function of height for 12-hour forecasts valid at 12Z on July 28, 2018. Control is in blue; experiment (with smoke clearing) is in red. The experiment bias has mean -0.1480 °C compared to the control's mean of -0.1483 °C; the experiment RMS has mean 1.044 °C compared to the control's mean of 1.043 °C. Verification is conducted against 75 radiosonde observations.



longitude for the 12-hour forecasts valid at 0 UTC (*Figure 3*) indicates that the smoke clearing indeed impacted heating during the daytime hours of model integration and overall improved the temperature forecast.

Conclusions and Future Work

The experiments described herein demonstrate that a simple AOD assimilation approach of removing spurious smoke concentrations from the HRRR can improve forecasts of environmental conditions related to smoke distributions. These results (along with Pagowski's variational DA experiments) suggest that using AOD to modify model smoke is a viable path forward for HRRR smoke field adjustment via AOD assimilation. Experiments including AOD in a variational approach will be conducted in an experimental HRRR configuration later in 2020.

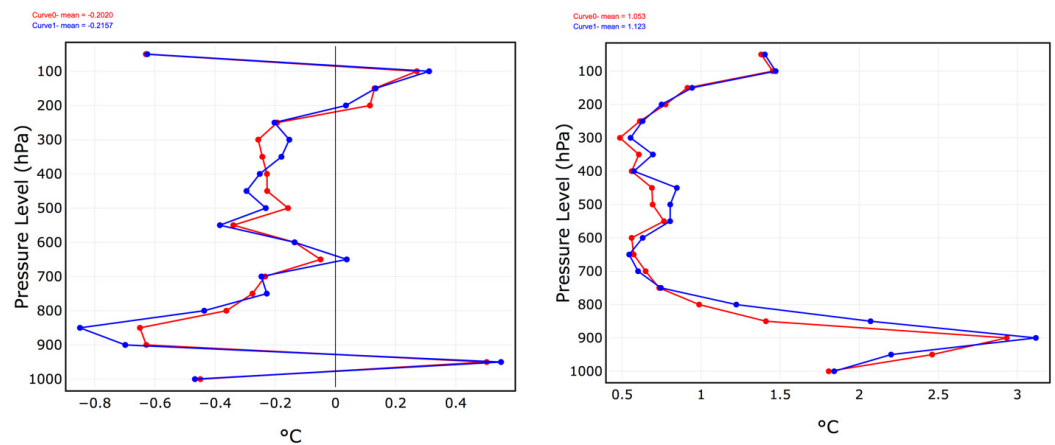
Many other upgrades to the Rapid Refresh smoke forecasting capability are also being considered. FRP and AOD from GOES-R satellites are expected to improve forecasts during intervals and in areas in which data

from polar-orbiting satellites are unavailable; feedback between the smoke tracer and the water- and ice-friendly aerosols in the Thompson microphysics scheme has been tested; modeled fire strength and horizontal extent may, in the future, be modulated by surrounding meteorology; potential improvements to the plume-rise algorithm will be studied; and more. In addition, an effort has been undertaken to numerically assess HRRR's smoke forecasts by converting the smoke concentration to simulated AOD for comparison with satellite AOD measurements (Xu et al., 2018).

Acknowledgments

The authors wish to acknowledge the contributions of Mariusz Pagowski, Chuanyu Xu, Curtis R. Alexander, and others to this effort. The authors thank NOAA's Joint Polar Satellite System (JPSS) Proving Ground and Risk Reduction Program for funding the RAP/HRRR-Smoke model development. Partial funding for this research was also provided by NOAA Awards NA19OAR4320073 and NA15OAR4320101.

Figure 3. Temperature bias (left) and RMS (right) as a function of height for 12-hour forecasts valid at 0Z on July 29, 2018. Control is in blue; experiment (with smoke clearing) is in red. The experiment bias has mean -0.2020 °C compared to the control's mean of -0.2157 °C; the experiment RMS has mean 1.053 °C compared to the control's mean of 1.123 °C. Verification is conducted against 70 radiosonde observations.



Authors

Amanda Back
 Colorado State University
 Cooperative Institute for Research in the
 Atmosphere
 at NOAA/OAR/GSL

Ravan Ahmadov
 University of Colorado Boulder
 Cooperative Institute for Research in
 Environmental Sciences
 at NOAA/OAR/ESRL/Global Systems
 Division

Eric P. James
 University of Colorado Boulder
 Cooperative Institute for Research in
 Environmental Sciences
 at NOAA/OAR/ESRL/Global Systems
 Division

Georg Grell
 NOAA/OAR/GSL
 325 Broadway
 Boulder, CO 80305-3337

Gabriel Pereira
 Federal University of Sao Joao del-Rei
 (UFSJ)
 Sao Joao del-Rei, Brazil

Saulo R. Freitas
 Universities Space Research Association
 Columbia, MD, USA and
 Global Modeling and Assimilation Office
 NASA/GSFC
 Greenbelt, MD, USA

Ivan A. Csiszar
 Satellite Meteorology and Climatology
 Division
 NOAA/NESDIS Center for Satellite

Applications and Research
 College Park, MD, USA

Marina Tsidulko
 NOAA/NESDIS Center for Satellite
 Applications and Research
 College Park, MD, USA

Shobha Kondragunta
 NOAA/NESDIS Center for Satellite
 Applications and Research, Satellite
 Meteorology and Climatology Division
 (STAR SMCD)
 College Park, MD, USA

References

Ahmadov, R. et al., 2017, Using VIIRS fire radiative power data to simulate biomass burning emissions, plume rise and smoke transport in a real-time air quality modeling system, 2017 IEEE International Geoscience and Remote Sensing Symposium (IGARSS), Fort Worth, TX, 2017, pp. 2806-2808. doi: 10.1109/IGARSS.2017.8127581.

Grell, G. A., Peckham, S. E., Schmitz, R., McKeen, S. A., Frost, G., Skamarock, W. C., and Eder, B.: Fully coupled "online" chemistry within the WRF model, *Atmos. Environ.*, 39, 6957-6975, 10.1016/j.atmosenv.2005.04.027, 2005.

Kondragunta, S., I. Laszlo, P. Ciren, H. Zhang, H. Liu, J. Huang, and A. Huff, 2017: *Exceptional events monitoring using S-NPP VIIRS aerosol products. 2017 IEEE International Geoscience and Remote Sensing Symposium (IGARSS)*, 1285-1287.

Ladwig, T. T., D. Dowell, and C. R. Alexander, 2019: Development and Improvements in the High Resolution Rapid Refresh

- Data Assimilation System (HRRRDAS). American Geophysical Union Fall Meeting, 9 Dec. 2019. Conference Presentation.
- Ladwig, T. T., D. C. Dowell, C. Alexander, M. Hu, S. Weygandt, S. Benjamin, and E. P. James, 2020: Assimilating Cloud Observations in the High Resolution Rapid Refresh Data Assimilation System (HRRRDAS). 24th Conference on Integrated Observing and Assimilation Systems for the Atmosphere, Oceans, and Land Surface, 16 Jan. 2020, 100th American Meteorological Society Annual Meeting. Conference Presentation.
- Pagowski, M., R. B. Pierce, G. A. Grell, R. Ahmadov, and S. A. McKeen, 2018: Assimilation of VIIRS AOD to Improve Smoke Forecasts over the Western United States. 20th Joint Conference of the Applications of Air Pollution Meteorology with the A&WMA, 10 Jan. 2018, 98th American Meteorological Society Annual Meeting. Conference Presentation.
- Xu, C., S. Kondragunta, R. Ahmadov, and E. James, 2018: Evaluation of HRRR Smoke Forecast using SNPP VIIRS Aerosol Products. American Geophysical Union Fall Meeting, 14 Dec. 2018. Poster Presentation.
- Zhou, L., M. Divakarla, X. Liu, A. Layns., and M. Goldberg, M, 2019: An overview of the science performances and calibration/validation of Joint Polar Satellite System Operational Products. *Remote Sensing*, 11(6), 698.

Impacts of Aerosols on Simulated Brightness Temperature and Analysis Fields

Motivations

Aerosols effects on radiation and cloud processes have been established in climate research for decades. More recently, aerosol effects have also been recognized to be important for numerical weather prediction. Tompkins et al. (2005), Rodwell and Jung (2008), Mulcahy et al. (2014), and Bozzo et al. (2017), to name a few, all demonstrated that the model forecast performance improved with a proper representation of aerosol information to the radiation or/and microphysics schemes within the forecast model; but compared to the attention of improving physical representation of aerosols in numerical models, the aerosol effects are rarely discussed in the context of data assimilation. Kim et al. (2018) investigated the impact of aerosols on the simulated brightness temperature (BT) using the GEOS-atmospheric data assimilation system (GEOS-ADAS) and found warmer analyzed temperature when considering aerosols in simulated BT derivation. The global data assimilation system (GDAS) in NCEP, however, does not consider any aerosol influences during the derivation of BT, which is manipulated

by the radiative transfer model. Therefore, the absence of aerosols may introduce errors into the analysis system. In this study, we examine the influences of aerosols on GDAS meteorological analysis by including aerosols into the radiance observation operator.

Experimental Design

In this study, experiments are conducted using the GDAS v14. All the experiments perform GSI-based 4DEnVar with 80 ensemble members on T254 every 6 hours for August 2017. In GSI, the observation operator for radiance sensors uses the Community Radiative Transfer Model (CRTM v2.2.4) developed by JCSDA. Three sets of experiments are listed as follows:

- CTL: the baseline aerosol-blind experiment
- AER: the offline aerosol-aware analysis experiment, which applies the short-range forecasts (3 – 9 hours) from CTL
- CAER: the fully cycled, aerosol-aware analysis experiment, which uses its own short-range forecasts.

Both CTL and CAER perform 120 hours of global forecast at 00Z, while AER only

generates analysis of every cycle. For aerosol-aware experiments, AER and CAER, the aerosol information is taken from NOAA Environmental Modeling System (NEMS) GFS Aerosol Component (NGAC) v2 (Wang et al., 2018). NGAC v2 is a global aerosol forecast system that consists of the NEMS GFS and Goddard Chemistry Aerosol Radiation and Transport (GOCART). The comparison between CTL and AER infers the aerosol influences on the system are isolated, while the comparison between CTL and CAER can reveal a more realistic impact of aerosol on the operational global NWP system.

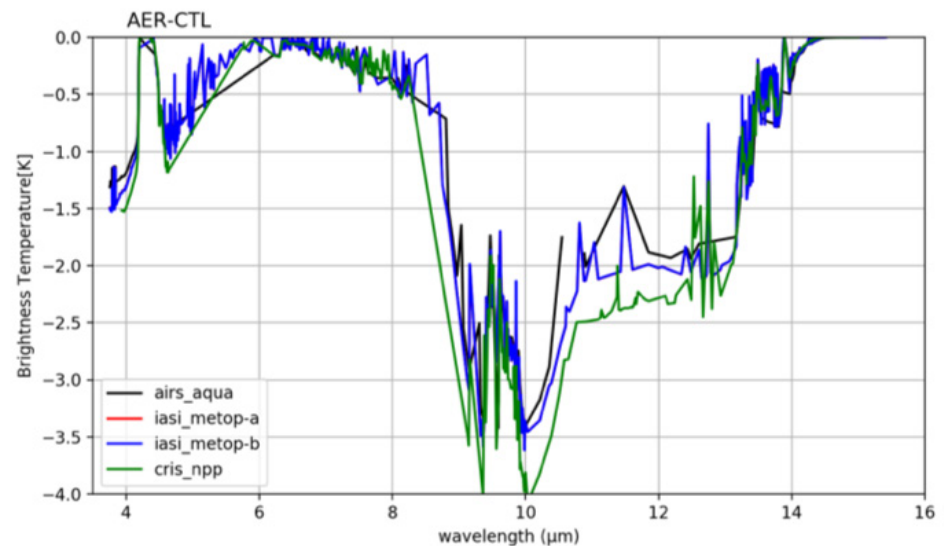
Results

In this article, a general assessment of aerosol impacts on the analysis is addressed through monthly statistics. A case study about the impacts of aerosol-aware analysis on the African easterly wave that developed Hurricane Harvey in 2017 is presented in this issue by Grogan and Lu (2020).

Aerosol Impact On Analysis

Figure 1 shows the simulated BT difference between CTL and AER for the hyperspectral

Figure 1. Simulated brightness temperature difference between AER and CTL of hyperspectral thermal infrared sensors averaged over dust dominant observations ($AOD > 0.3$, dust AOD fraction $> 65\%$).



infrared sensors over dust dominant regions. The figure clearly shows reductions in the BTs across the thermal window region (8–14 μm), which is consistent with Matricardi (2005) and Kim et al. (2018). With the inclusion of the aerosol information in AER, these reductions are anticipated because aloft aerosols would attenuate the upward terrestrial radiation that reaches satellite sensors. The reduction of BT of satellite measurement due to aerosols has been discussed in Sokolik (2002). *Figure 2* displays the mean and RMS of the first guess departure on BT for AER and CTL, which are taken from the Infrared Atmospheric Sounding Interferometer (IASI) on METOP-A over dust dominant regions before quality control and bias correction. Given the cooling on the BT in *Figure 1*, AER introduces more positive first guess departure in the thermal window. This means AER produces a warmer first guess departure than CTL. However, AER shows larger RMS across some thermal window channels, which may be due to inaccuracies in the aerosol modeling or from

the cold biases in meteorological forecasts. *Figure 3* displays the difference between CTL and AER for the sea surface temperature and the temperature at 850 mb. Over the Atlantic Ocean, where the dominant aerosol type is Saharan dust, the figure depicts that more positive first guess departure introduces warmer sea surface temperature (SST) analysis. Comparisons of the fields with buoy measurements indicate that the warmer SSTs over Atlantic Ocean are in better agreement with observations (not shown here). It also generates warmer analysis temperatures in the lower atmosphere over North Africa and the transatlantic region near the equator, but cooler analysis temperature occurs near the coast of Africa. These features are consistent with Kim et al. (2018)

Forecast Skill of Aerosol-aware Analysis

The model forecast performance for the fully-cycled, aerosol-aware analysis experiment (CAER) is examined using the NCEP/EMC forecast verification package.

Figure 2. Mean (left) and RMS (right) first guess departure of IASI on METOP-A averaged over $\text{AOD} > 0.3$ and dust AOD fraction $> 65\%$ observations during Aug 1 to 28, 2017.

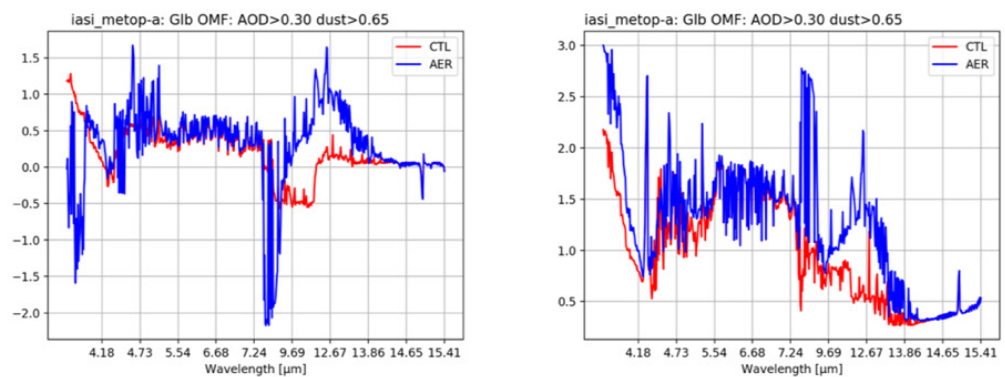


Figure 3. Monthly mean analysis difference of sea surface temperature (left panel) and 850 hPa temperature (right panel) between AER and CTL.

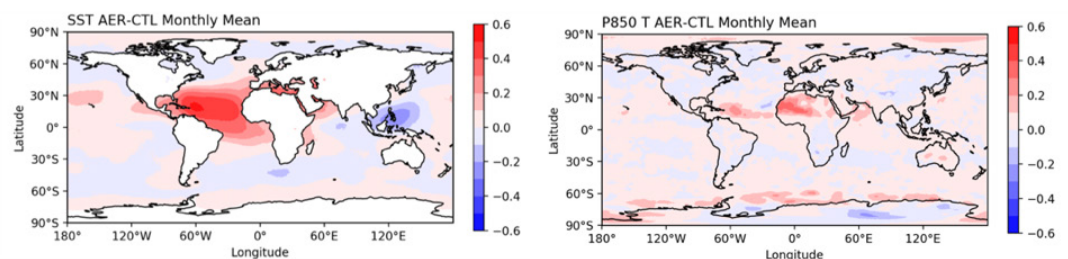


Figure 4 displays the scorecard of anomaly correlation and RMSE for the day--1 to 5 forecasts. It should be noted that the forecasts of CAER have better agreement with its own analysis in upper levels in the northern hemisphere (20 °N – 80 °N) than CTL. There is, however, no significant improvement or degradation in the southern hemisphere (20 °S – 80 °S). Compared to both hemispheres, CAER shows a more positive impact in the tropical region (20 °S – 20 °N), which may

be due to the larger aerosol loading in this region.

Summary

GDAS experiments are conducted to investigate the aerosol impacts on simulated BT, analysis fields, and following forecasts. With the inclusion of the aerosol information in the radiance observation operator of the analysis system, the simulated BTs in dust dominant regions are reduced in the thermal

Figure 4. Scorecard of anomaly correlation and RMSE of comparison between CAER and CTL. Green means CAER is better than CTL at 95% (filled box), 99% (▲), and 99.9% (▲) significance level. Red means CAER is worse than CTL at 95% (filled box), 99% (▼), and 99.9% (▼) significance level. Grey boxes mean no statistically significant difference between CAER and CTL. Blue boxes are not statistically relevant. The statistics are calculated between 20 to 80 degrees of latitude for both hemispheres. The data between 20 °S and 20 °N is used for the tropical region.

		N. Hemisphere				S. Hemisphere				Tropics				
		Day 1	Day 3	Day 5	Day 6	Day 1	Day 3	Day 5	Day 6	Day 1	Day 3	Day 5	Day 6	
Anomaly Correlation	Heights	250hPa	M	M	M	M	M	M	M	M				
		500hPa				M	M	M	M	M				
		700hPa				M				M				
		1000hPa				M	M	M	M	M				
	Vector Wind	250hPa	M	M	M	M				M				
		500hPa				M				M				
		850hPa				M				M				
	Temp	250hPa				M	M	M	M	M				
		500hPa	M	M	M	M		▼		M				
		850hPa	M	M	M	M				M				
	MSLP	MSL	M	M	M	M	M	M	M	M				
	RMSE	Heights	10hPa		▲	▲	M				M	▲	▲	▲
20hPa			▲	▲	▲	M				M	▲	▲	▲	M
50hPa			▲	▲	▲	M	▲			M	▲	▲	▲	M
100hPa			▲	▲		M	▲	▲		M	▲	▲	▲	M
200hPa						M				M		▲	▲	M
500hPa						M				M	▲	▲	▲	M
700hPa						M				M				M
850hPa						M				M		▲	▲	M
1000hPa						M				M		▲	▲	M
Vector Wind		10hPa	▲	▲	▲	M				M	▲	▲	▲	M
		20hPa	▲	▲	▲	M		▲		M	▲	▲	▲	M
		50hPa	▲	▲	▲	M	▲			M	▲	▲	▲	M
		100hPa	▲	▲		M	▲	▲		M	▲	▲	▲	M
		200hPa	▲			M	▲			M	▲			M
		500hPa				M				M	▲	▲		M
		700hPa				M				M				M
		850hPa				M				M	▲	▲		M
		1000hPa				M				M	▲	▲		M
Temp		10hPa	▲			M				M	▲	▲	▲	M
		20hPa	▲	▲	▲	M				M	▲	▲	▲	M
		50hPa	▲	▲	▲	M	▲			M	▲	▲	▲	M
		100hPa	▲	▲		M	▲			M	▲	▲	▲	M
		200hPa				M	▲			M	▲	▲	▲	M
		500hPa				M				M			▼	M
	700hPa				M				M	▲			M	
	850hPa	▲			M				M	▲			M	
	1000hPa	▲			M				M	▲	▲		M	

infrared window region (8 – 14 μm). The off-line aerosol aware experiment (AER) produces a warmer first guess departure but also a larger RMS for the first guess departure. As a consequence, AER generates warmer SST in the Atlantic Ocean; warmer lower atmosphere over Africa and the transatlantic region. But cooler temperature analysis occurs over the Atlantic Ocean near the coast of Africa. The warmer SST in the Atlantic Ocean has better agreement with buoy measurements.

From the verification scorecard, neutral to positive results of fully-cycled, aerosol-aware experiment (CAER) are revealed. It should be noted that CAER shows better performance in the tropical region and upper level in the northern hemisphere than in the southern hemisphere. Although the promising results are shown in this article, the aerosol information from the free forecasts of NGAC v2 could introduce errors into the analysis system, because the aerosol information is treated as the truth under the current configuration. Therefore, the bias correction and quality control should be revisited for better utilization of modeling aerosol information in the meteorological data assimilation.

Acknowledgments

The work presented here is supported by NOAA NWS NGGPS R2O (Award number #NA15NWS468008). The project is a collaborative effort from UAlbany (Cheng-Hsuan Lu, Shih-Wei Wei, Sheng-Po Chen, Dustin Grogan), NCEP/EMC (Robert Grumbine, Andrew Collard, Jun Wang, Partha Bhattacharjee, Bert Katz, Xu Li), and NESDIS/STAR (Quanhua Liu, Zhu Tong). The GDAS experiments were conducted at UW-Madison SSEC's S4 cluster.

Authors

Shih-Wei Wei
University at Albany, State University of
New York

Andrew Collard
IMSG at NOAA/NCEP/EMC

Robert Grumbine
NOAA/NCEP/EMC

Quanhua Liu
NOAA/NESDIS/STAR

Cheng-Hsuan (Sarah) Lu
University at Albany, State University of
New York
Joint Center for Satellite Data Assimilation

References

- Bozzo, A., S. Remy, A. Benedetti, J. Flemming, P. Bechtold, M. J. Rodwell, and J.-J. Morcrette, 2017: Implementation of a CAMS-based aerosol climatology in the IFS. *ECMWF Tech Memo*. 801
- Grogan D. and C.-H. Lu, 2020: Impacts of Aerosols on Meteorological Assimilation: A Case Study for the African Easterly Wave that Develops Hurricane Harvey, *JCSDA Quarterly*, 66, Spring 2020 (this issue).
- Kim, J., S. Akella, A. M. da Silva, R. Todling, and W. McCarty, 2018: Preliminary evaluation of influence of aerosols on the simulation of brightness temperature in the NASA's Goddard Earth Observing System Atmospheric Data Assimilation System. *Technical Report Series on Global Modeling and Data Assimilation*, NASA/TM-2018-104606/ Vol. 49

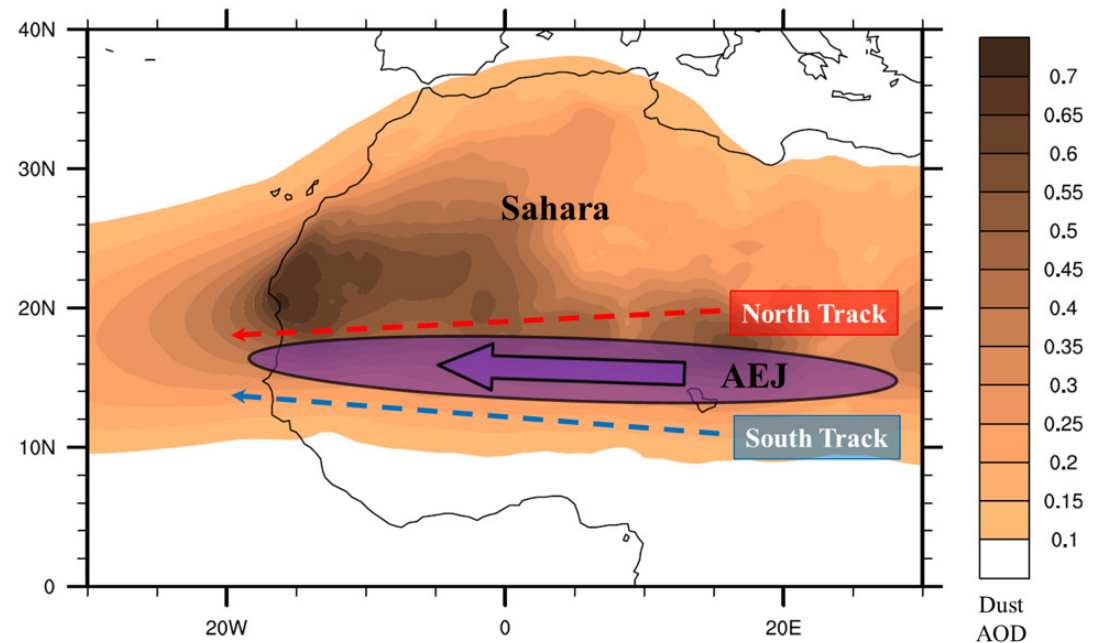
- Matricardi, M., 2005: The inclusion of aerosols and clouds in RTIASI, the ECMWF fast radiative transfer model for the infrared atmospheric sounding interferometer. *ECMWF Tech. Memo.* 474
- Mulcahy, J. P., D. N. Walters, N. Bellouin, and S. F. Milton, 2014: Impacts of increasing the aerosol complexity in the Met Office global numerical weather prediction model. *Atmospheric Chemistry and Physics*, 14, 4749–4778, <https://doi.org/10.5194/acp-14-4749-2014>.
- Rodwell, M. J., and T. Jung, 2008: Understanding the local and global impacts of model physics changes: an aerosol example. *Quarterly Journal of the Royal Meteorological Society*, 134, 1479–1497, <https://doi.org/10.1002/qj.298>.
- Sokolik, I. N., 2002: The spectral radiative signature of wind-blown mineral dust: Implications for remote sensing in the thermal IR region: THE SPECTRAL RADIATIVE SIGNATURE OF WIND-BLOWN MINERAL DUST. *Geophysical Research Letters*, 29, 7-1-7-4, <https://doi.org/10.1029/2002GL015910>.
- Tompkins, A. M., 2005: Influence of aerosol climatology on forecasts of the African Easterly Jet. *Geophysical Research Letters*, 32, <https://doi.org/10.1029/2004GL022189>.
- Wang, J., P. S. Bhattacharjee, V. Tallapragada, C.-H. Lu, S. Kondragunta, A. da Silva, X. Zhang, S.-P. Chen, S.-W. Wei, A. S. Darmanov, J. McQueen, P. Lee, P. Koner, and A. Harris, 2018: The implementation of NEMS GFS Aerosol Component (NGAC) Version 2.0 for global multispecies forecasting at NOAA/NCEP – Part 1: Model descriptions. *Geoscientific Model Development*, 11, 2315–2332, <https://doi.org/10.5194/gmd-11-2315-2018>.

Impacts of Aerosols on Meteorological Assimilation: A Case Study for the African Easterly Wave that Developed Hurricane Harvey

Motivation

North Africa is the largest source of atmospheric aerosols on Earth. Each year, the Saharan Desert emits massive amounts of mineral dust, which can form vast plumes that span thousands of kilometers. In summer, these large-scale plumes interact with African easterly waves (AEWs), which are the prominent synoptic-scale disturbances over the region. The AEW structure typically consists of two circulation centers that reside on either side of the African easterly jet (AEJ) (*Figure 1*). The southern circulation peaks at mid-levels (800-600

Figure 1. Schematic showing the dust aerosol optical depth (AOD) climatology during summer. Overlaid are the zonally-averaged AEJ and the tracks of the AEW.



hPa) and is frequently coupled to convection, while the northern circulation peaks at low-levels (900-700 hPa) and is immersed in Saharan dust. The two circulations often merge into a single circulation center over the East Atlantic that can produce a favorable environment for tropical cyclogenesis (Ross and Krishnamurti, 2007).

Grogan and Thorncroft (2019) used MERRA-2 reanalysis fields to examine the mean characteristics of AEWs that are coupled to dust over North Africa and the East Atlantic. They showed that the structure of the dust-coupled AEWs differ from previously studied convectively-coupled AEWs (e.g., Kiladis et al., 2006) in that they possess stronger northern circulations. They also showed that the enhanced northern circulation is connected to diabatic energy processes due to the radiative heating of dust anomalies that are transported by the AEWs. The influence of this eddy dust radiative feedback has been shown in several studies to have modest impacts on the energetics and dynamics

of AEWs (Grogan et al., 2016, 2017, 2019; Bercos-Hickey et al., 2017; Nathan et al., 2017). Given that this feedback is driven by large-scale dust anomalies, the proper representation of aerosols, including their episodic nature, is crucial to fully capture the aerosol radiative effects in models.

Currently, the NCEP's operational Global Forecast System (GFS) model includes the radiative effects of aerosols by using prescribed monthly climatologies from the Optical Properties of Aerosol and Clouds (OPAC) software package (Hess et al., 1998), while the Global Data Assimilation System (GDAS) does not consider the impact of aerosols on radiances. Consequently, the climatologies lack the episodic nature of aerosols, while the assimilation increasingly relies on quality control and bias correction procedures in aerosol-rich regions, such as North Africa.

In this study, we use GDAS to include aerosol information into the radiance observation. Through this effort, we hypothesize that

the aerosol radiative effects are better represented within the meteorological fields of the analysis, which subsequently improves the forecasts of AEWs. This is tested for the AEW circulation that developed Hurricane Harvey in August 2017.

Experimental Design

To assess the aerosols impacts, we conducted two sets of experiments. The first experiment was an aerosol blind run (CTL), which used the default settings of GDAS v14. The second experiment was an aerosol aware run (CAER), which incorporated aerosol information into GDAS each analysis cycle. To incorporate the aerosols, 3D mixing ratios for all species (dust, sea-salt, organic carbon, and black carbon) were ingested into the radiance observation operator within the Community Radiative Transfer Model (CRTM v2.2.4) to influence brightness temperatures. The aerosol mixing ratios were obtained by running the NEMS GFS Aerosol Component (NGAC v2) model (Wang et al., 2018). CAER is also a fully cycled run that uses its own short-range forecasts (3-9 hours) as its first guess. For more details on the experimental design and the aerosol impact on brightness temperatures, see Wei et al. (2020) from this issue.

Results

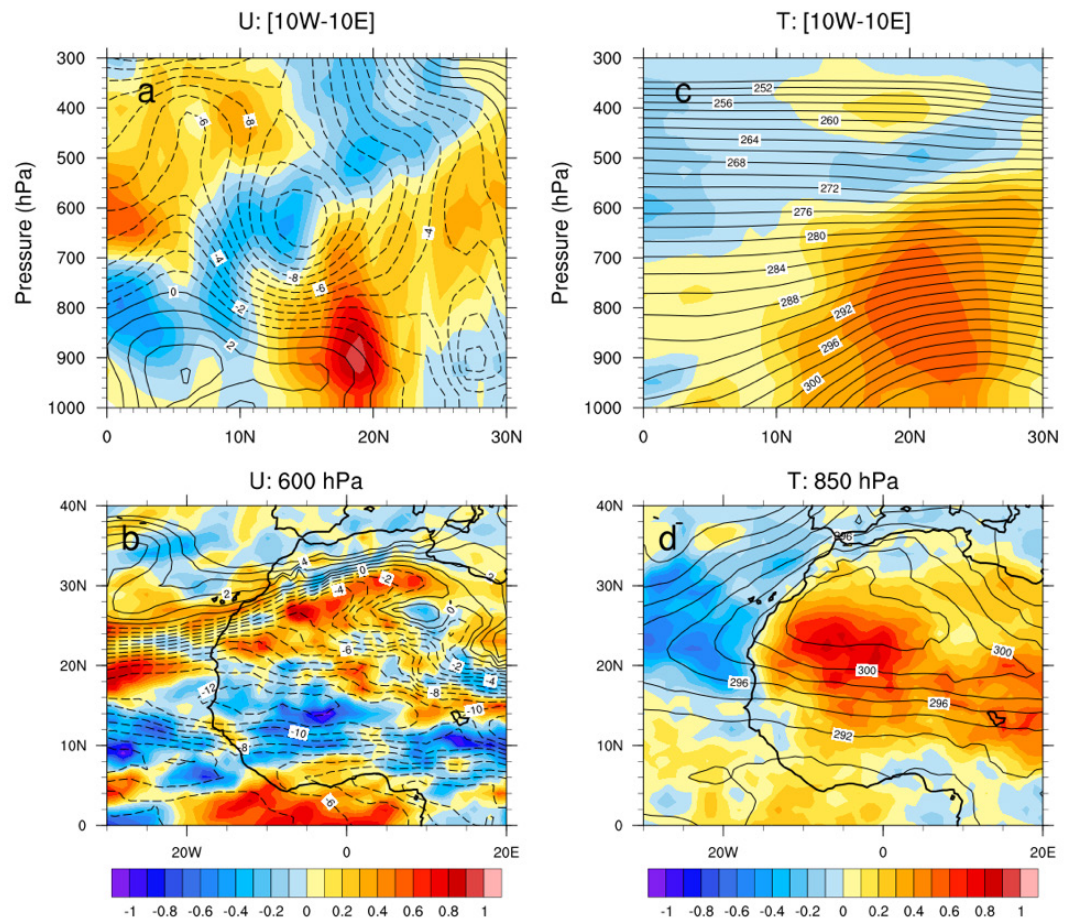
We will first examine the environmental differences of the atmosphere from the analysis fields over North Africa and the East Atlantic during August 2017. Then our focus will turn to the AEW case, where we will examine the analysis and forecasts for the two experiments.

Time averages of the zonal-wind and temperature from CTL (*Figure 2, contours*) accurately capture the main summertime

features over the region. For example, the zonal-wind shows the AEJ is at mid-levels (*Figure 2a*: 15°N, 600 hPa) and extends across North Africa and the East Atlantic (*Figure 2b*: 10-15°N, 20W-25°E), while the warm temperatures over the Sahara set up the strong meridional temperature gradients below the AEJ core in the Sahel (*Figures 2c and 2d*: 10-20°N, 1000-650 hPa). The CAER-CTL differences (*Figure 2, colors*) show that the aerosol impacts accelerate the AEJ core by ~0.5 m/s across the majority of North Africa and the Eastern Atlantic (blues in *Figure 2a*, 650 hPa, 15°N and *Figure 2b*, 10-15°N, 20E-30°W), accentuate warming in the Sahara and the Sahel by ~0.5 K (*reds in Figures 2c and 2d*, 10-30°N), and cool the marine layer by ~0.5 K off the coast of the Saharan Desert (*blues in Figure 2d*, 15-30°W, 15-30°N). These responses to the wind and temperature infer that for CAER, the aerosol radiative effects have increased in the boundary layer (~1000-600 hPa) over North Africa and in the Saharan Air Layer (~800-600 hPa) over the East Atlantic.

Hurricane Harvey, which made landfall along the Middle Texas Coast on August 25th, began as an AEW with two cyclonic circulations east of the Greenwich Meridian on August 7th. The streamlines over North Africa (*Figure 3*) show that the two circulations (Xs) traveled west and merged into a single circulation over the East Atlantic on August 12th. During this time, the mid-level vorticity from each circulation intensified (*Figure 3a*), reached peak amplitude (*Figure 3b*), decayed near the coast (*Figure 3c*), and then re-intensified slightly after the two circulations merged over the East Atlantic (*Figure 3d*). The resulting AEW, however, did not develop the named storm Harvey until August 17th.

Figure 2. Horizontal and vertical plots of the CTL analysis (contours) and the CAER-CTL analysis difference (colors) of the (a, b) zonal-wind, U , and (b, c) temperature, T . The vertical sections (top) are zonally-averaged from $10^{\circ}W - 10^{\circ}E$, while horizontal sections (bottom) are taken at specified pressure levels. Contour/color units: (a,b) m/s and (c, d) $^{\circ}K$. The fields are computed from July 29th – August 28th.



To examine the aerosol impacts on the wave in the analysis fields, the colors in Figure 3 show the CAER-CTL difference in the 850 hPa cyclonic vorticity. From August 9th – 11th, CAER increases the cyclonic vorticity of the northern circulation (reds at $20^{\circ}N$) and decreases the vorticity of the southern circulation (blues at $12^{\circ}N$). The impacts were largest during August 9th – 10th, which are the times when the amplitudes of the vorticity centers peaked. The structural changes to the AEW are consistent with the intensity difference shown for the vorticity over North Africa for the entire month (not shown). Moreover, these results are consistent with the impacts of the eddy dust radiative feedback on the energetics and dynamics AEWs, which has been exposed in idealized studies (e.g., Grogan et al., 2016, 2019).

Given the aerosol-induced changes to the AEW structure in the analysis fields, we next explored the forecasting of the wave downstream. To do this, we computed the CAER-CTL Root-Mean-Square-Error (RMSE) for the 950-650 hPa vorticity following the AEW. The RMSEs were computed for every 24-hour forecast initialized from August 8th – 11th (Table 1). The Table shows that CAER generally improves the forecasting of the AEW vorticity structure (green numbers). The “most improved” forecast occurred on August 10th, which showed reductions in RMSE for each forecast day. During this initialization time, the differences in the vorticity centers were largest in the analysis fields (e.g., colors in Figure 3b). Therefore, when the aerosol radiative effects

Figure 3. 850 hPa streamlines from August 9th – August 12th (a-d). The wave locations from the tracking algorithm are marked with Xs using the tracking algorithm described in Brammer and Thorncroft (2015). Overlaid is the CAER-CTL difference in 850 hPa relative vorticity (colors). To reduce clutter, the colors are only shown when the CTL flow is cyclonic and the CAER-CTL difference is more than $\pm 0.5 \times 10^{-5} \text{ s}^{-1}$.

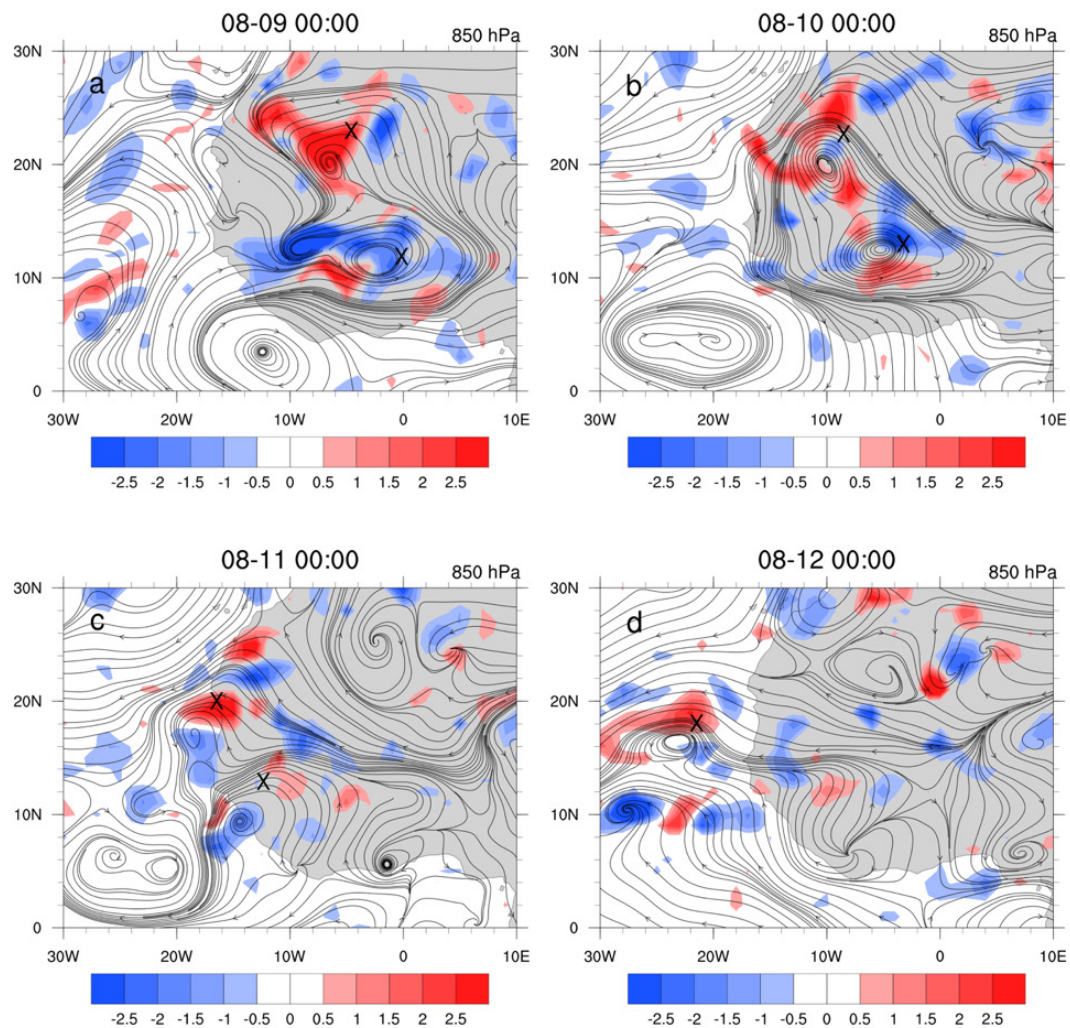


Table 1. RMSE differences in the 950-650 hPa relative vorticity between CAER and CTL forecasts. The green values indicate CAER improved the forecast, while red values indicate CAER degraded the forecast; crossed-out values were not significant to the 99% confidence interval. For each forecast day, the RMSE differences were computed following the AEW (i.e., the latitudes were fixed at 5-25°N while a 10° longitude window shifted west with the circulations in time).

INITIALIZATION	1 DAY	2 DAY	3 DAY	4 DAY	5 DAY
AUGUST 8TH	0.25	0.28	1.38	2.12	4.48
AUGUST 9TH	0.17	0.64	0.89	1.27	0.08
AUGUST 10TH	1.02	1.28	0.68	1.94	0.85
AUGUST 11TH	0.85	0.18	2.46	0.34	0.04

from the assimilation begins to enact large circulation changes in the analysis fields, the corresponding forecasts further improve the AEW’s downstream behavior.

Summary

In this study, we examined the impact of including aerosol information on the radiance observation operator in GDAS. In

particular, we investigated the impacts of Saharan mineral dust on an AEW, and its environment, over North Africa and the East Atlantic during August 2017. The AEW of interest developed Hurricane Harvey and had a representative two-circulation structure over North Africa.

We conducted two sets of GDAS experiments: one aerosol blind run (CTL), which used the default configuration, and one aerosol aware run (CAER), which considered the aerosol mixing ratios in the radiance observation operator. Analysis differences of the environmental zonal-wind and temperature showed that CAER increased the AEJ, warmed the Sahara and Sahel throughout the boundary layer, and cooled the marine layer over the East Atlantic, which is due to increases in the aerosol radiative effects on the environment. Analysis differences in the structure of the AEW of interest showed that CAER strengthened the northern circulation and weakened the southern circulation, which are consistent with the changes induced by the eddy dust radiative feedback on the dynamics of AEWs.

To assess the aerosol impacts on the forecast performance of the AEW circulation, the RMSE in vorticity was computed for the 5-day forecasts initialized over North Africa (August 8th – August 11th). The differences showed that CAER generally improved the forecasts of the AEW downstream, especially for times initialized with large differences in the structure of the AEW circulations. Forecast improvements such as these can be crucial for determining the timing and intensity of developing TCs that originate from AEWs.

This study demonstrates that the incorporation of aerosol information into the meteorological assimilation better represents the aerosol radiative effects on synoptic-scale AEWs. Therefore, including aerosol information in the assimilation step may be a viable approach for a future operational setting.

Acknowledgements

The work presented here is supported by NOAA NWS NGGPS R2O (Award number #NA15NWS468008). The project is a collaborative effort from UAlbany (Cheng-Hsuan Lu, Shih-Wei Wei, Sheng-Po Chen, and Dustin Grogan), NCEP/EMC (Robert Grumbine, Andrew Collard, Jun Wang, Partha Bhattacharjee, Bert Katz, Xu Li), and NESDIS/STAR (Quanhua Liu, Zhu Tong). The GDAS experiments were conducted at UW-Madison SSEC's S4 cluster.

Authors

Dustin Grogan
University at Albany, State University of
New York

Cheng-Hsuan (Sarah) Lu
University at Albany, State University of
New York
Joint Center for Satellite Data Assimilation

References

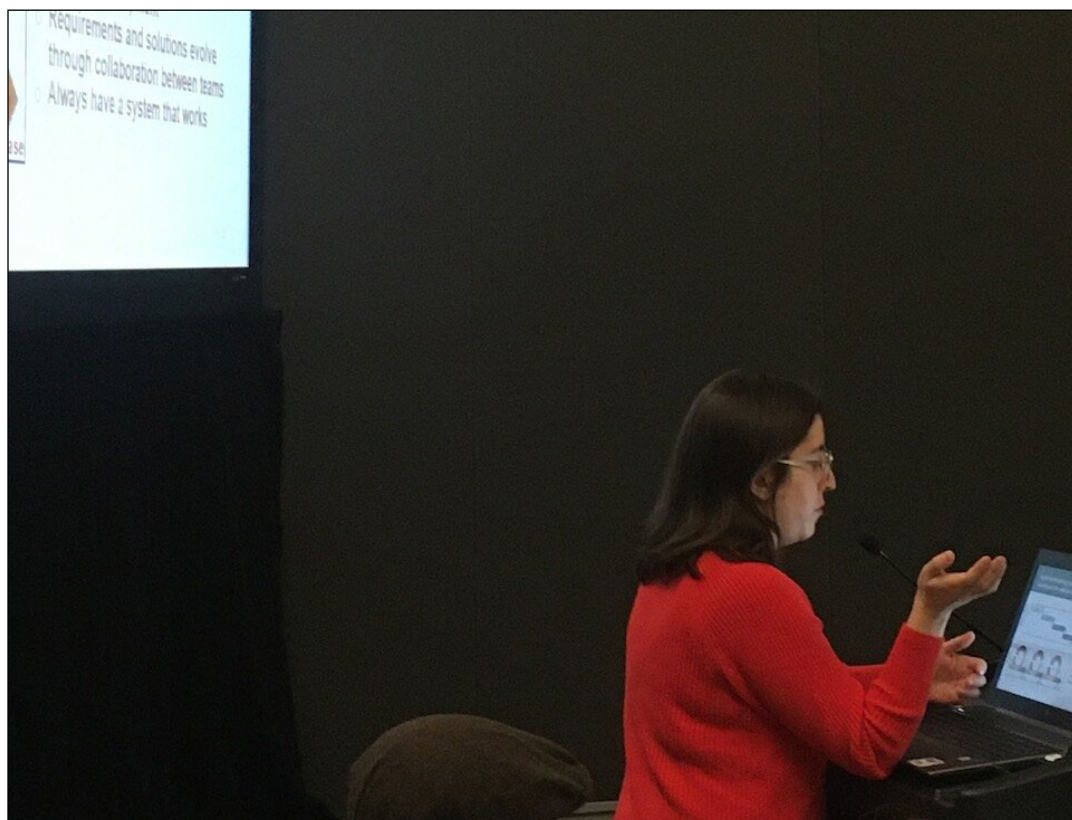
Bercos-Hickey E., T.R. Nathan, and S.-H. Chen, 2017: Saharan dust and the African easterly jet–African easterly wave system: structure, location and energetics. *Q. J. R. Meteorol. Soc.*, 143, 2797-2808. <https://doi.org/10.1002/qj.3128>.

- Brammer A., and C.D. Thorncroft, 2015: Variability and evolution of African easterly wave structures and their relationship with tropical cyclogenesis over the eastern Atlantic. *Mon. Wea. Rev.* 143, 4975-4995. <https://doi.org/10.1175/MWR-D-15-0106.1>.
- Ross, R. and T.N. Krishnamurti, 2007: Low-Level African Easterly Wave Activity and Its Relation to Atlantic Tropical Cyclogenesis in 2001. *Mon. Wea. Rev.*, 135, 3950-3964. <https://doi.org/10.1175/2007MWR1996.1>.
- Grogan D.F.P., T.R. Nathan, and S.-H. Chen, 2016: Effect of Saharan dust on the linear dynamics of African easterly waves. *J. Atmos. Sci.* 73, 891-911. <https://doi.org/10.1175/JAS-D-15-0143.1>.
- Grogan D.F.P., T.R. Nathan, and S.-H. Chen, 2017: Saharan dust and the nonlinear evolution of the African easterly jet–African easterly wave system. *J. Atmos. Sci.* 74, 24-47. <https://doi.org/10.1175/JAS-D-16-0118.1>.
- Grogan D.F.P. and C.D. Thorncroft, 2019: The characteristics of African easterly waves coupled to Saharan mineral dust aerosols. *Q. J. R. Meteorol. Soc.* 2019, 1–17. <https://doi.org/10.1002/qj.3483>.
- Grogan, D.F.P., T.R. Nathan, and S.-H. Chen, 2019: Structural Changes in the African Easterly Jet and Its Role in Mediating the Effects of Saharan Dust on the Linear Dynamics of African Easterly Waves. *J. Atmos. Sci.* 76, 3359-3365. <https://doi.org/10.1175/JAS-D-19-0104.1>.
- Hess, M.P., P. Koepke, and I. Shult, 1998: Optical properties of aerosol and clouds: The software package OPAC. *Bull. Amer Meteor. Soc.*, 79, 831-844. [https://doi.org/10.1175/1520-0477\(1998\)079<0831:OP OAAC>2.0.CO;2](https://doi.org/10.1175/1520-0477(1998)079<0831:OP OAAC>2.0.CO;2).
- Kiladis G.N., C.D. Thorncroft, and N.M.J. Hall, 2006. Three-Dimensional Structure and Dynamics of African Easterly Waves. Part I: observations. *J. Atmos. Sci.* 63, 2212-2230. <https://doi.org/10.1175/JAS3741.1>.
- Nathan T.R., D.F.P. Grogan, and S.-H. Chen, 2017: Subcritical destabilization of African easterly waves by Saharan mineral dust. *J. Atmos. Sci.* 74, 1039-1055. <https://doi.org/10.1175/JAS-D-16-0247.1>.
- Wang, J., et al., 2018: The implementation of NEMS GFS Aerosol Component (NGAC) Version 2.0 for global multispecies forecasting at NOAA/NCEP– Part 1: Model descriptions, *Geosci. Model Dev.*, 11, 2315–2332. <https://doi.org/10.5194/gmd-11-2315-2018>.
- Wei S.-W., A. Collard, R. Grumbine, Q. Liu, and C.-H. Lu, 2020: Impacts of aerosols on meteorological assimilation: Aerosol impact on simulated brightness temperature and analysis fields. *JCSDA Quarterly*, 66, Spring 2020 (this issue).

MEETING REPORT

8th AMS Symposium on the Joint Center for Satellite Data Assimilation

Dr. Maryam Presenting during the 8th Annual Meeting of the American Meteorological Society (AMS) Symposium on the Joint Center for Satellite Data Assimilation.



The JCSDA was proud to host its 8th Symposium at the Annual Meeting of the American Meteorological Society (AMS) in Boston, MA, January 12–17, 2020. This was the 100th meeting for the AMS, and consequently a very well-attended one. The participation of US federal government employees, many of whom were furloughed and unable to take part in the 99th AMS Annual meeting, may also have swelled the ranks and clearly increased the energy and excitement of the gathering.

In total, there were 755 sessions and over 4300 presentations, counting both talks and posters. Indeed, it was challenging to attend as many of the presentations as one would like; with parallel sessions, every attendee had to make difficult choices on a regular basis. The JCSDA was fortunate then, to hold its symposium on Tuesday, January 14; though there were compelling alternative sessions, it may have been the most well-attended day overall, and the JCSDA posters and talks received a great deal of attention. Note that many of the presentations are recorded and available online from the AMS meeting website, so there is still an opportunity for our audience to see ones they missed.

The symposium program was organized into five oral sessions, as well as a poster session. The first oral session was chaired by Kevin Garrett of NESDIS/STAR and was devoted to Land, Ocean, and Cryosphere DA. Daryl Kleist (NWS/NCEP) and Guillaume Vernieres (JCSDA) co-chaired the second oral session, on New Contributions to the Community Radiative Transfer Model (CRTM.) Jim Yoe (NCEP and JCSDA) and Ben Johnson (JCSDA) co-chaired the last oral session of the morning, on Contributions to the Joint Effort for Data assimilation Integration (JEDI).

For many the lunch break was no break at all, as there were multiple AMS Town Hall meetings of interest to the JCSDA community. These included a NOAA Modeling Forum, a discussion of the USAF's Weather Capabilities Roadmap, and a meeting devoted to NASA Science and Space Weather - among others.

The symposium was rounded out in the afternoon with an oral session on Assimilation of Aerosol Observations chaired by Ron Gelaro (NASA) and Yannick Tremolet (JCSDA) and one on the Assimilation of New Observations, with Ben Ruston (NRL) and Jim Yoe at the podium. The ensuing poster session was lively and well attended.

PEOPLE

Welcome Dr. Cheng Dang



Cheng Dang joined the JCSDA in Boulder, CO, in January 2020, as a project scientist with the Community Radiative Transfer Model (CRTM) core team. Her primary responsibility and focus include improving the representation of aerosol species and their solar optical properties in CRTM for a better constraint on AOD and irradiance data assimilation and exploring other scientific questions revolving around aerosol radiative effects.

Cheng obtained her Ph.D. degree in Atmospheric Sciences from the University of Washington in 2017, researching the radiative impact of light-absorbing particles (LAPs) in snow. During her Ph.D. study, she participated in a two-month field campaign to sample the LAPs in snow, which were analyzed in labs by spectrophotometer and chemical experiments for the LAP concentration and species. She then studied the radiative effects of observed LAPs in the snow with various assumptions of snow optical properties. After graduation, Cheng joined the Department of Earth System Science of the University of California, Irvine, to improve the solar radiative simulation of snow, sea ice, and aerosols in the Energy Exascale Earth System Model (E3SM). She developed a hybrid radiative transfer model that can be applied to any cryospheric surface in the Earth system models for efficient and accurate simulation of cryosphere solar radiative properties. Now, Cheng is excited to explore the scientific potentials of CRTM.

Apart from science, Cheng loves movies, traveling, and exploring the ocean as deep as her diving license permits.

EDITOR'S NOTE

Every three months when I am reminded it's time to prepare a note for the Newsletter, I have a bit of anxiety. I fret about having nothing new to say, and about putting down words that are stale and which do not adequately reflect the energy, excitement, and accomplishment of the JCSDA and its community. Sometimes, I wish for the chance to inject a little more drama into the column. Now I have to laugh a bit, and remind myself of the adage that we should be careful what we wish for.

Today virtually everyone participating in the mission of the JCSDA, whether core staff, in-kind contributor, agency partner or sponsor, or from the academic community, is teleworking as part of the national imperative to practice social distancing to protect ourselves, our families, and communities by slowing the spread of the COVID-19 virus. Our priorities and notions of work-life balance are being revised as a matter of necessity. I expect that everyone feels some degree of anxiety, both personally and professionally, wondering when our lives and work will return to normal, and indeed, how normal will be different in the aftermath of the pandemic. That's enough drama for anyone, I am sure.

Among our activities most likely to be impacted are those that do not lend themselves to remote participation. Given prohibitions on traveling and large-group gatherings, the JCSDA has canceled the Annual Technical Review Meeting and Science Workshop that was to have been held June 2–4, 2020. We already are working to schedule the 2021 Workshop at the United States Air Force Academy in Colorado Springs, CO, and will share dates and details as they become firm. In the meantime, we are committed to providing and enhancing our interactions with the internal and external scientific community, through our quarterly review and all-hands meetings, and via the JCSDA Symposium as part of the AMS Annual Meeting in January, 2021.

Code sprints that had been planned for the Spring and early Summer either have been or are likely to be postponed. Please be sure to check the JCSDA Website for the most current status of planned events.

Despite the challenges and uncertainty we are adjusting and persevering. Many of us, of course, already were teleworking on at least a partial basis, and are aware of the benefits and demands of doing so. Others are learning fast, and as a geographically distributed center, we long have been accustomed to distant collaboration. It is heartening to see the determination to move forward at every level of the Joint Center in these times, to do the scientific and technical work for which we are known.

Three examples of that work are included in this issue, focusing on assimilation of atmospheric aerosol data assimilation. Each of these articles is based on work that was presented as part of the poster session for the JCSDA Symposium at the Annual Meeting of the American Meteorological Society in January, 2020. I thank the authors for their willingness to expand those presentations to share with the Quarterly readership.

As always, I hope that you find this edition interesting and informative. And I hope that it finds you and yours well in every sense of the word. I know that we will all continue to do good work as we ride out the present storm; I encourage everyone to take care of themselves and their families as they do so, and to take care of one another as best we can.

SCIENCE CALENDAR

UPCOMING EVENTS

Calendar dates and information are accurate as of publish date. Please check event websites for updates.

MEETINGS OF INTEREST

DATE	LOCATIONS	WEBSITE	TITLE
Postponed. Date and other details To Be Determined.	Fort Collins, CO	http://www.isac.cnr.it/~ipwg/	IPWG
Postponed until September 14–18.	Fort Collins, CO	https://www.cira.colostate.edu/conferences/8th-international-symposium-on-data-assimilation/	8th International Symposium on Data Assimilation (ISDA)
July 19–24, 2020	Waikoloa, Hawaii	https://igarss2020.org/	IGARSS
September 28–October 2, 2020	Wurzburg, Germany	https://www.eumetsat.int/website/home/News/ConferencesandEvents/DAT_4635627.html	EUMETSAT Meteorological Satellite Conference 2020
October 18–23, 2020	Banff	https://www.birs.ca/events/2020/5-day-workshops/20w5166	Mathematical Approaches for Data Assimilation of Atmospheric Constituents and Inverse Modeling
December 7–11, 2020	San Francisco, California	https://www.agu.org/	AGU
January 10–14, 2021	New Orleans, Louisiana	https://www.ametsoc.org/index.cfm/ams/	AMS

MEETINGS AND EVENTS SPONSORED BY JCSDA

DATE	LOCATIONS	WEBSITE	TITLE
Canceled.	Canceled	jcsda.org/events	18th JCSDA Technical Review Meeting and Science Workshop

CAREER OPPORTUNITIES

Opportunities in support of JCSDA may be found at <https://www.jcsda.org/opportunities> as they become available.